Dynamics in the Plasma Chamber for E157

R. Govil, D. Whittum and J. Wurtele

In this note we sumarize the known beam dynamics issues appropriate for the parameters of the E157 experiment,[1] and we go on to derive some new results that should be helpful in determining beam-phase space after passage through the plasma. First we review the scaling laws for a relativistic electron beam propagation in plasma.[2] We go on to set down a simple formalism for beam optics, in the *magnetically self-focused* regime (overdense plasma), as appropriate for the beam head in E157. Optics for portions of the beam in the *ion-focused regime* (underdense plasma) have been noted by Assmann, *et al.*,[3] and we review these. Transverse beam dynamics with the plasma-electron coupled wakefield is then checked analytically, and with a macroparticle model. Finally, all results together are checked with the help of a particle-in-cell simulation.[4]

1. Introduction

The problem of interest is depicted in Fig.1. We inject a beam with input phase-space parameters as listed in Table 1 (assumed known), and ask, given plasma parameters as in Table 2, what are the outgoing phase-space characteristics of the beam? These tables also serve to define some notation we will be using.

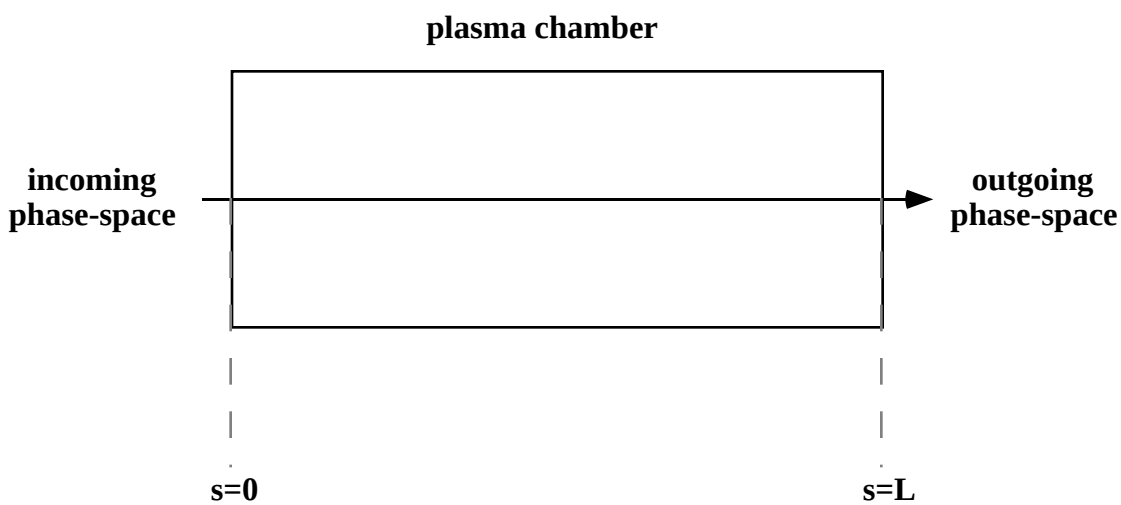

FIGURE 1. We are interested in determing the evolution of beam phase-space for a high-energy electron beam in a plasma tank, as for E157 parameters.

[1] T. Katsouleas, *et al.*, "A proposal for a 1 GeV plasma-wakefield acceleration experiment at SLAC", *Proceedings of the 1997 Particle Accelerator Conference* (IEEE, New York, to be published).

[2] D. H. Whittum, "Continuous plasma final focus", in *Nonlinear and Relativistic Effects in Plasmas*, V. Stefan, ed., (AIP, New York, 1992) pp. 387-401. (reissued as an ARDB Tech. Note).

[3] R. Assmann, *et al.*, "Proposal for a One GeV Plasma Wakefield Acceleration Experiment at SLAC".

[4] D.H. Whittum, "Transverse two-stream instability of a beam with a Bennett profile", Phys. Plasma **4** (1997) 1154.

Table 1. Electron beam parameters for E157. The nominal operating point corresponds to the underlined values.

particles in the bunch	N_b	$3.0 - \underline{4.0} \times 10^{10}$
bunch length (rms)	σ_z	$\underline{0.6} - 1.1$ mm
rms normalized *x*-emittance	$\varepsilon_{\mathrm{nx}}$	$\underline{6} - 4 \times 10^{-5}$ mrad
rms normalized *y*-emittance	$\varepsilon_{\mathrm{nx}}$	$\underline{1.5} - 4 \times 10^{-5}$ mrad
beam position (rms jitter)	x_b, y_b	50 μm
initial rms beam *x*-size	σ_x	$25 - 100\,\mu$m
initial rms beam *y*-size	σ_y	$25 - 100\,\mu$m
beam energy	E_b	$30 - \underline{46.6} - 52$ GeV
rms fractional momentum spread	σ_δ	$\underline{0.2} - 1\%$

Table 2. Plasma parameters for E157. Nominal operating values are underlined.

plasma chamber length	L	$\underline{1.0} - 1.5$ m
plasma density	n_p	$10^{14} - \underline{5 \times 10^{14}} - 10^{15}$ cm^{-3}
Rayleigh length, ionizing laser	L_R	2.7 m
radius of laser spot	r_L	300 μm

In the estimates that follow we will consider an injected beam described by a Gaussian beam with number density

$$n_b(x,y,\zeta) = \frac{Q_b}{(2\pi)^{3/2}\sigma_x\sigma_y\sigma_z}\exp\left(-\frac{x^2}{2\sigma_x^2} - \frac{y^2}{2\sigma_y^2} - \frac{\zeta^2}{2\sigma_z^2}\right), \qquad \text{(injected)}$$

where the "beam-coordinate" $\zeta = ct - z$, and we approximate the beam drift velocity by c, the speed of light, not being concerned for the moment with radiative effects. The beam charge is Q_b. The incoming peak beam density is then

$$n_{b0} = \frac{Q_b}{(2\pi)^{3/2}\sigma_x\sigma_y\sigma_z}.$$

We may also wish to refer to the beam current waveform,

$$I_b(\zeta) = \frac{Q_b c}{(2\pi)^{1/2}\sigma_z}\exp\left(-\frac{\zeta^2}{2\sigma_z^2}\right),$$

and the peak current

$$I_{b0} = \frac{Q_b c}{(2\pi)^{1/2}\sigma_z}.$$

For the plasma, we will refer to the plasma wavenumber

$$k_p = \sqrt{4\pi n_p r_e},$$

where (in cgs units) $r_e = e^2/mc^2 \approx 2.82\times10^{-13}$cm is the classical electron radius, -*e* is the electron charge, and *m* is the electron mass. The angular plasma frequency is $\omega_p = k_p c$. These quantities are listed in Table 3, for the nominal parameters. Initial peak beam density is listed corresponding to $\sigma_x = \sigma_y = 50\ \mu$m and $N_b = 4\times10^{10}$. This number is somewhat adjustable obviously, and the matter of beam density will be discussed more below.

Table 3. Nominal derived parameters for E157.

beam charge	Q_b	$4.8-\underline{6.4}$ nC
peak beam current	I_{b0}	$0.5-\underline{1.3}$ kA
initial peak number density	n_{b0}	1.7×10^{15} cm^{-3}
inverse plasma wavenumber	k_p^{-1}	$53-\underline{38}-17\,\mu$m
adiabatic current rise parameter	$k_p\sigma_z$	21 - 11
Lorentz factor	γ	9.12×10^4

2. Regimes of propagation

Let us review the regimes of propagation of interest. The overall picture is that of Fig. 2. The three regimes of propagation of primary interest for this experiment are illustrated in Fig. 3. The fourth regime corresponds to $n_p < n_b/\gamma^2$ ("*forgot to backfill the chamber regime*"), and, while interesting, is postponed until we come to an enumeration of the various operating scenarios.

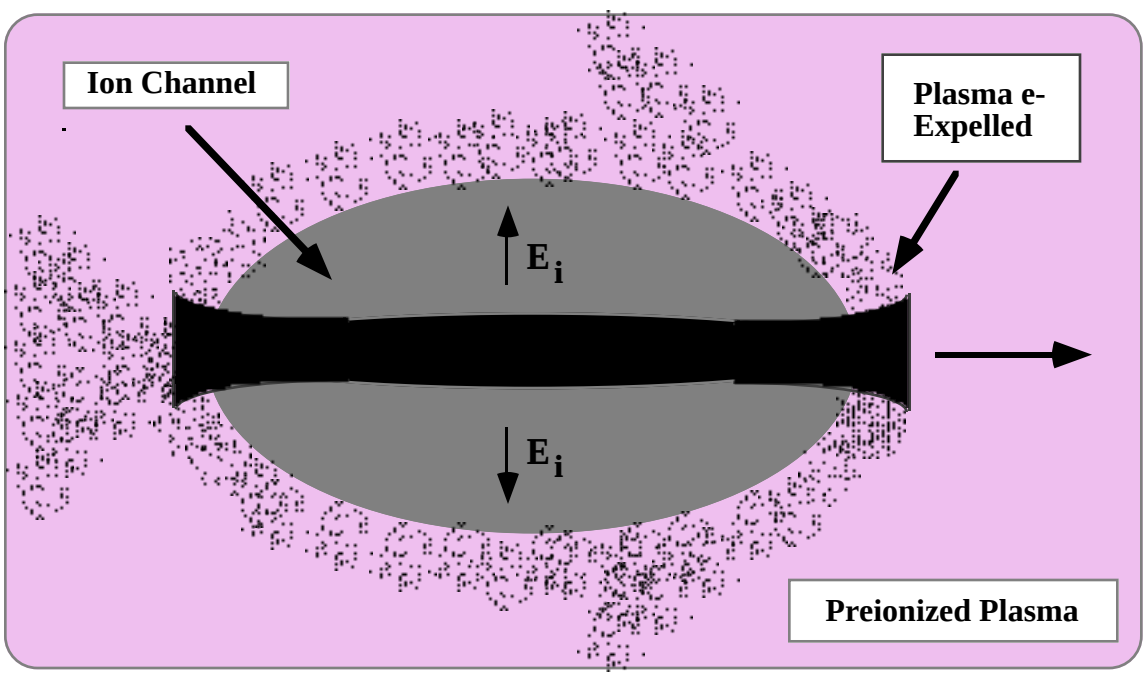

FIGURE 2. The radial electric field of the relativistic electron beam expels plasma electrons from a large volume, or "channel". Beam electrons are then focused by the radial electric field of the relatively immobile ions.

In this section, we put aside the matter of the longitudinal wakefield, as it is a higher order effect in the experiment (even while it is central to the goals of the

experiment). We concentrate exclusively on transverse beam dynamics, and associated "zeroth-order" concerns. When speaking of the injected beam, we will be picturing a long Gaussian bunch with $\sigma_x = \sigma_y = \sigma_r$. "Long" means $k_p \sigma_z >> 1$. We enumerate the regimes of propagation, starting from the highest plasma densities and working toward the lowest. There are two criteria by which to gauge the plasma density, one is the ratio n_p / n_b and the other is $k_p \sigma_r$.

Current Neutralization Regime (Overdense Plasma)

A collisionless plasma will oppose the current flow corresponding to an injected electron beam.[5] One can guess this from Lenz's Law, or one can infer it, realizing that a collisionless plasma behaves like an inductive element (due to the intertial phase-lag in the electron motion), so that the beam head must lose energy, and therefore must be doing work on plasma electrons. The plasma electrons however are only able to resolve spatial features on the length scale k_p^{-1}; this is to say that plasma return currents extend through a transverse volume of this dimension. In the limit $k_p \sigma_r > 1$, these plasma return currents are flowing through the bulk of the beam, as opposed to a volume much larger than the beam, and in this limit, the net magnetic field within the beam is diminished. In this limit too, the plasma will be more dense than the beam so that electric fields will be neutralized. As a result the net transverse force experienced by the beam is simply its own magnetic field, diminished somewhat by the contribution of the plasma electrons. This regime is accessible in E157 only in the case of an expanded incoming beam, and plasma density at the high end of the nominal parameters. While it is in principle possible to access this regime in the E157 experiment, we will omit further discussion of it here.

Magnetically Self-Focused Regime (Overdense Plasma)

When the plasma is denser than the beam---a condition that always applies for some portion of the beam head---the beam electric field expels only a fraction of the plasma electron charge, enough so that the resulting surfeit of ion-charge is adequate to cancel the electric field of the beam. In this limit, the net charge density is approximately zero, and the only field component remaining is the magnetic field due to the beam. This we may compute from Ampere's Law,

$$\frac{1}{r}\frac{\partial}{\partial r} r B_{b\theta} = -4\pi e n_{b0} \frac{V}{c} \exp\left(-\frac{r^2}{2\sigma_r^2}\right),$$

with beam drift speed $V \approx c$. The solution is

$$B_{b\theta} = -4\pi e n_{b0} \frac{\sigma_r^2}{r} \frac{V}{c} \left\{1 - \exp\left(-\frac{1}{2}\frac{r^2}{\sigma_r^2}\right)\right\},$$

and the net force on a beam electron is given by

[5] D. H. Whittum, A. M. Sessler, J. J. Stewart, and S. S. Yu, "Plasma suppression of beamstrahlung", Particle Accelerators **34**, 89 (1990).

$$F_r = -e\left(E_r - \frac{V}{c}B_{b\theta}\right) \approx -4\pi e^2 n_{b0}\frac{\sigma_r^2}{r}\left\{1-\exp\left(-\frac{1}{2}\frac{r^2}{\sigma_r^2}\right)\right\}$$

$$\approx -mc^2 k_{b0}^2 \frac{\sigma_r^2}{r}\left\{1-\exp\left(-\frac{1}{2}\frac{r^2}{\sigma_r^2}\right)\right\},$$

where we introduce the beam wavenumber,

$$k_{b0} = \left(4\pi n_{b0} r_e\right)^{1/2} = \left(4\pi \frac{I_{b0}/ec}{2\pi\sigma_r^2} r_e\right)^{1/2} = \left(2\frac{I_{b0}}{I_0}\right)^{1/2}\frac{1}{\sigma_r} = \frac{\left(2\nu_b\right)^{1/2}}{\sigma_r}.$$

The equivalent forms listed are helpful in appreciating the dependence on beam-size. Here $I_0 = mc^3/e \approx 17\,\text{kA}$, and $\nu_b = I_{b0}/I_0$ is Budker's parameter. For $\sigma_r = 50\,\mu\text{m}$, $\sigma_z = 0.6\,\text{mm}$, and 4×10^{10} beam electrons, $n_{b0} \approx 1.7\times10^{15}\,\text{cm}^{-3}$ and $k_{b0} \approx 77.5\,\text{cm}^{-1}$, scaling in inverse proportion to the beam size (which, as we will see, should not be viewed as a static quantity). Paraxially,

$$\frac{d\vec{p}_\perp}{dt} = F_r\hat{r} \approx -\frac{1}{2}mc^2 k_{b0}^2\,\vec{r}_\perp, \qquad \Leftrightarrow \qquad \frac{d}{dz}\gamma\,\vec{r}_\perp{}' \approx -\frac{1}{2}k_{b0}^2\,\vec{r}_\perp.$$

This may be expressed in various conventional forms as

$$K = \frac{1}{2\gamma}k_{b0}^2 \qquad \text{or} \qquad k_\beta^2 = \frac{1}{2\gamma}k_{b0}^2 = \frac{1}{\sigma_r^2}\left(\frac{\nu_b}{\gamma}\right). \qquad \text{(magnetically self-focused regime),}$$

The ratio ν_b/γ will be recognized as the ratio of beam current to Alfven current. Note the implication that $k_\beta\sigma_r << 1$.

We will return later to consider more generally the self-pinched behavior, including the aberrations characteristic of this self-focusing force. In the meantime, we may note simply that for $\sigma_r = 50\,\mu\text{m}$, the natural self-pinched betatron period is $\lambda_\beta = 2\pi/k_\beta = 5.5\,\text{cm}$, using $\gamma \approx 9.12\times10^4$ as for 46.6 GeV. This number is useful in that it allows one to gauge that the beam will have plenty of time, over the course of 1 m of plasma, to self-pinch and scallop, if mismatched. This simple calculation is not a substitute for a detailed calculation of the beam envelope behavior (see below) as a function of the beam coordinate ζ, and the displacement through the chamber, *s*.

In passing let us note the equilibrium self-pinched beam-size, for a initially matched beam, absent scattering and other sources of incoherence. Normalized emittance is constant,

$$\varepsilon_n = \gamma k_\beta \sigma_r^2 = \gamma\frac{1}{\sigma_r}\left(\frac{\nu_b}{\gamma}\right)^{1/2}\sigma_r^2 = \left(\nu_b\gamma\right)^{1/2}\sigma_r, \qquad \text{(MFR equilibrium)}$$

so that

$$\sigma_{eq} = \frac{\varepsilon_n}{\left(\nu_b\gamma\right)^{1/2}}, \qquad k_\beta = \frac{1}{\sigma_r}\left(\frac{\nu_b}{\gamma}\right)^{1/2} = \frac{\left(\nu_b\gamma\right)^{1/2}}{\varepsilon_n}\left(\frac{\nu_b}{\gamma}\right)^{1/2} = \frac{\nu_b}{\varepsilon_n}. \qquad \text{(MFR equilibrium)}$$

For a round-beam emittance of $\varepsilon_n \approx 4\times10^{-5}$ m – rad, $\gamma \approx 9.12\times10^4$ (as for 46.6 GeV) and for $v_b/\gamma \approx 8.4\times10^{-7}$ ($I_{b0} \approx 1.3$ kA as for $N_b \approx 4\times10^{10}$ and $\sigma_z = 0.6$ mm) one finds an equilibrium beam-size of $\sigma_{eq} \approx 0.48\,\mu$m. However, this assumes a plasma density at least as great as the corresponding beam density

$$n_b = \frac{I_{b0}/ec}{2\pi\sigma_r^2} = \frac{v_b}{2\pi\sigma_r^2 r_e}.$$

This corresponds to $n_b \approx 1.9\times10^{19}\,\mathrm{cm}^{-3}$, far higher than plasma densities envisioned for E157. Thus if the beam peak is to reach equilibrium, it will not be in the magnetically self-focused regime.

Ion-Focused Regime (Underdense Plasma)

As the beam head propagates through the plasma, it continuously expels some plasma electrons from the beam volume. If the beam density is sufficiently high that $n_b > n_p$ then a region near the beam-axis is completely denuded of plasma electrons, forming an "ion-channel". This region may in fact be much larger than the beam. This circumstance will occur for nominal E158 parameters, within 1-2 σ_z of the beam peak. One can estimate the radius of this channel by considering the electric field computed from Poisson's equation,

$$\frac{1}{r}\frac{\partial}{\partial r} rE_{br} = -4\pi e n_{b0} \exp\left(-\frac{r^2}{2\sigma_r^2}\right),$$

with solution

$$E_{br} = -4\pi e n_{b0} \frac{\sigma_r^2}{r}\left\{1-\exp\left(-\frac{1}{2}\frac{r^2}{\sigma_r^2}\right)\right\}.$$

Meanwhile, a uniform column of singly-charged ions of number density n_p provides an electric field

$$E_{ir} = 2\pi e n_p r.$$

The beam and ion electrostatic fields subtract to give zero at some radius R, the "neutralization radius", satisfying

$$2\pi e n_p R = 4\pi e n_{b0} \frac{\sigma_r^2}{R}\left\{1-\exp\left(-\frac{1}{2}\frac{R^2}{\sigma_r^2}\right)\right\},$$

or

$$\frac{\left(\frac{1}{2}\frac{R^2}{\sigma_r^2}\right)}{\left\{1-\exp\left(-\frac{1}{2}\frac{R^2}{\sigma_r^2}\right)\right\}} = \frac{n_{b0}}{n_p}.$$

For a very underdense plasma, $n_{b0}/n_p >> 1$, and the radius of this channel is given by

$$R \approx \sigma_r \left(2\frac{n_{b0}}{n_p} \right)^{1/2} .$$

In the case of adiabatic current rise, $k_p \sigma_z >> 1$, as for E157, one may picture plasma electrons being adiabatically expelled beyond this radius. They are also accelerated backwards, at the expense of work done by the beam head. This backward component of the electron motion corresponds to a return current carried by the plasma electrons. This return current sheath extends radially with a radial e-folding length of k_p^{-1} beyond the ion-channel.[6] Note the implication that a wall-current monitor encircling the interaction chamber should detect negligible wall return current when the plasma is on. If a beam position monitor should be in some manner filled with plasma at this density, it too would not produce a detectable signal.

The tranvserse force witnessed by a beam electron in the IFR takes the form,

$$F_r = -e\left(E_{ir} + E_{br} - \frac{V}{c} B_{b\theta} \right) \approx -eE_{ir} - e\frac{1}{\gamma^2} E_{br} \approx -eE_{ir} \approx -\frac{1}{2} mc^2 k_p^2 r .$$

Paraxially or not this may be expressed as

$$\frac{d\vec{p}_\perp}{dt} = F_r \hat{r} \approx -\frac{1}{2} mc^2 k_p^2 \vec{r}_\perp , \qquad \Leftrightarrow \qquad \frac{d}{dz} \gamma \vec{r}_\perp' \approx -\frac{1}{2} k_p^2 \vec{r}_\perp .$$

This may be expressed in various conventional forms as

$$K = \frac{1}{2\gamma} k_p^2 \qquad \text{or} \qquad k_\beta^2 = \frac{1}{2\gamma} k_p^2 . \qquad \text{(ion-focused regime),}$$

Let us note the condition for equilbrium propagation. Neglecting scattering and other incoherent effects, the normalized emittance is a constant,

$$\varepsilon_n = \gamma k_\beta \sigma_r^2 = \gamma \frac{k_p}{(2\gamma)^{1/2}} \sigma_r^2 = \left(\frac{\gamma}{2} \right)^{1/2} k_p \sigma_r^2 ,$$

thus the equilibrium beam-size is

$$\sigma_{eq} = \left(\frac{2}{\gamma} \right)^{1/4} \left(\frac{\varepsilon_n}{k_p} \right)^{1/2} . \qquad \text{(ion-focused equilibrium)}$$

Note that this is independent of beam current (provided the assumption $n_b >> n_p$ holds), and thus could apply uniformly along the mid-section of the beam. For a round-beam emittance of $\varepsilon_n \approx 4 \times 10^{-5}$ m – rad, $\gamma \approx 9.12 \times 10^4$ (as for 46.6 GeV), and for the nominal plasma density $n_p \approx 5 \times 10^{14}$ cm^{-3}, $k_p^{-1} \approx 38\,\mu$m and we find $\sigma_{eq} \approx 2.7\,\mu$m. The corresponding equilibrium beam density is

[6] D. H. Whittum, "Nonlinear, relativistic return current sheath for an ion-focused beam" Phys. Fluids **B 4**, 476 (1992) .

$$n_b = \frac{v_b}{2\pi\sigma_r^2 r_e} \approx 6.1\times 10^{17}\ \text{cm}^{-3},$$

and this is consistent with the assumption of underdense propagation over a few σ_z of the beam, for E157 parameters. The corresponding channel radius is $R \approx 1.3\times 10^2\,\mu\text{m}$. The betatron period is $\lambda_\beta \approx 1.6\,\text{cm}$.

3. Higher-Order Effects

In this section we apply the scaling laws set down in Ref. 2 to summarize some of the nuisances associated with using a plasma.

Scattering

The total cross-section for small angle scattering is[7]

$$\sigma_s = \pi\left(\frac{2Zr_e}{\gamma}\right)^2 \frac{1}{\theta_{\min}^2}.$$

For a fully ionized, quasineutral plasma, $\theta_{\min} = \hbar / mc\gamma\lambda_D$, where λ_D is the Debye wavelength. However, for a partially ionized gas from which plasma electrons have been ejected, $\theta_{\min} = \hbar / mc\gamma R$, for scattering from ions, and $\theta_{\min} = \hbar / mc\gamma\, a$ for scattering from neutral atoms. The atomic number is Z and $a \approx 1.4\, a_B Z^{-1/3}$, is the screening radius in the Thomas-Fermi model (0.5 Å for lithium, $Z = 3$). The constant $\hbar = h/2\pi$, h is Planck's constant, and a_B is the Bohr radius, $a_B = \hbar^2 / me^2$. The mean-square scattered angle per scattering event is

$$\left\langle \theta^2 \right\rangle = 2\theta_{\min}^2 \ln\left(\frac{\theta_{\max}}{\theta_{\min}}\right).$$

The maximum scattering angle is $\theta_{\max} = \hbar / mc\gamma\, r_n$ where $r_n \approx 0.5\, r_e\, A^{1/3}$ is the nuclear radius and A is the mass number. (These are $r_n \approx 3\times 10^{-13}\,\text{cm}$ and $A \approx 6.941$ for lithium.) This gives, for scattering from neutrals,

$$\frac{\theta_{\max}}{\theta_{\min}} \approx \frac{5.26\times 10^4}{(AZ)^{1/3}} \approx 1.9\times 10^4,$$

or $\ln\left(\theta_{\max}/\theta_{\min}\right) \approx 10$, evaluating the result for lithium. For scattering from ions, in an unneutralized channel of radius R,

$$\frac{\theta_{\max}}{\theta_{\min}} \approx \frac{R}{r_n} \approx 5\times 10^{10},$$

and we evaluate the result for a $1.3\times 10^2\,\mu\text{m}$ channel of unneutralized lithium ions. This corresponds to $\ln\left(\theta_{\max}/\theta_{\min}\right) \approx 25$. In the following it will be assumed that the ionization

[7] J. D. Jackson, *Classical Electrodynamics*, 2nd ed. (Wiley, New York, 1975).

fraction, *f*, is unity, and that scattering with ions dominates.

The rms scattering angle after traversing a length *z*, $\Theta_{rms}(z)$, varies according to,

$$\frac{d}{dz}\Theta_{rms}^2 = n_p\,\sigma_s\left\langle \theta^2 \right\rangle = 8\pi\, n_p \frac{Z^2 r_e^2}{\gamma^2}\ln\left(\frac{\theta_{\max}}{\theta_{\min}}\right).$$

Emittance growth is then given by,[8]

$$\frac{d\varepsilon_n}{dz} = \frac{\gamma}{2\,k_\beta}\frac{d}{dz}\Theta_{rms}^2,$$

The change in normalized emittance in passing through the cell is then

$$\Delta\varepsilon_n = 2\, r_e Z^2 \int_0^{L_p} dz\, k_\beta \ln\left(\frac{\theta_{\max}}{\theta_{\min}}\right) \approx 4\pi\, \frac{L_p}{\lambda_\beta} r_e Z^2 \ln\left(\frac{\theta_{\max}}{\theta_{\min}}\right).$$

For a length $L_p \approx 1\,\mathrm{m}$ of lithium, and $\lambda_\beta \approx 1.6\,\mathrm{cm}$ as for $n_p \approx 5\times 10^{14}\ \mathrm{cm}^{-3}$ and 46.6 GeV, we have $\Delta\varepsilon_n \approx 2\times 10^{-11}\,\mathrm{m-rad}\times \ln\left(\theta_{\max}/\theta_{\min}\right)$. Thus emittance growth from scattering is negligible.

Beam-Induced Ionization

Ionization by the beam is of concern in determining the actual axial plasma density profile. Ionization is produced by the beam through electron impact,[9] gas breakdown, stripping of atoms and ions in the strong radial electric field at the beam "edge", or tunneling in the presence of this field. To accurately compute the net volume rate of ionization one could solve detailed rate equations, modelling of the chemistry of the particular gas used. In this section, only a few simple estimates are made.

The time scale for ionization in the overdense regime via impact ionization of neutrals by beam electrons and associated secondary electrons is[10] $\tau_b \approx 1/n_0\sigma_{bi}c$, with $\sigma_{bi} \approx 10^{-18}\,\mathrm{cm}^2$ and this is on the order of 30 ns at a plasma density of $10^{15}\,\mathrm{cm}^{-3}$, corresponding to negligible ionization by this mechanism. This scaling is modified by secondary electron multiplication (breakdown), an effect scaling with *E/p*, the ratio of radial electric field to pressure.[11] As a check of this effect one can compute the time for one secondary electron accelerated in the beam field, to ionize one neutral, $\tau_e \approx 1/n_0\sigma_{ei}V_e$, where σ_{ei} is the cross-section for ionization by secondaries and V_e is the secondary velocity. The quantity $\sigma_{ei}V_e$ peaks at secondary electron energies of order ~ 100 eV, with $\sigma_{ei}V_e \approx 10^{-7} - 10^{-8}\,\mathrm{cm}^3/\mathrm{sec}$, depending on the gas.[12] For densities in the range of $10^{15}\,\mathrm{cm}^{-3}$, this time scale $\tau_e \approx 10\,\mathrm{ns}$, quite long, amounting to a negligible effect.

---

[8] B. W. Montague and W. Schnell, in *Laser Acceleration of Particles*, edited by Chan Joshi and Thomas Katsouleas, AIP Conf. Proc. **130**, (AIP, New York, 1985), p. 146.

[9] D.P. Murphy, M. Raleigh, R.E. Pechacek, and J. R. Grieg, Phys. Fluids **30**, 232 (1987).

[10] A. E. S. Green, Radiation Research **64**, 119 (1975); A. E. S. Green and T. Sawada, J. Atmos. Terr. Phys. **34**, 1719 (1972).

[11] P. Felsenthal, J. M. Proud, Phys. Rev. **139**, 1796 (1965).

[12] M. Mitchner and C. H. Kruger, Jr., *Partially Ionized Gases*, (Wiley, New York).

The radial electric field at the beam edge will be adequate to strip an atomic electron with ionization potential, $\Delta\varepsilon$, for currents of order

$$I \approx \alpha^4 \frac{\sigma_r}{r_e}\left(\frac{\Delta\varepsilon}{e^2/a_B}\right) I_0 .$$

For very fine beams, this mechanism may fully ionize a channel larger than the beam, with some multiple ionization. In more practical units we may express this as

$$\Delta\varepsilon \approx 0.8\,\mathrm{eV}\,\frac{I(\mathrm{kA})}{\sigma_r(\mu\mathrm{m})},$$

and for $\sigma_r \approx 2.7\,\mu\mathrm{m}$ and $I \approx 1.3\,\mathrm{kA}$, this gives $\Delta\varepsilon \approx 0.4\,\mathrm{eV}$. The first ionization potential for lithium is 5.392 eV, and thus electrons are classically bound despite the strong fields. Tunneling is of course still present to some degree.[13] [incorporate tunneling rate in next revision]

In the meantime, plasma electrons are also lost through recombination on a time scale $\tau_r \approx 1/\alpha_r n_p$, and through attachment on a time scale $\tau_a \approx 1/\alpha_a n_0$. Here, α_r and α_a are the recombination and attachment coefficients, respectively.[14] Taking recombination in N_2 as an example, $\alpha_r \approx 2\times10^{-7}\,\mathrm{cm^3/s}$, at electron energies ~ 1 eV.[15] At a density of $10^{15}\,\mathrm{cm^{-3}}$, $\tau_r \approx 6\,\mathrm{ns}$ and this is quite long. (In fact, α_r will be lower for more energetic electrons.)

Generic Instabilities

A number of effects complicate the simple equilibrium pciture outlined above, and in this section, the time scales are noted. In the focusing cell, the equilibrium discussed so far, consisting of a beam travelling down a static channel, is maintained only to the extent that ions are immobile. In fact, ions at radius R collapse inward, neutralizing the beam charge, on a time scale,

$$\tau_{ion} \approx \frac{1}{4}\frac{R}{c}\left(\frac{m_i}{m}\right)^{1/2}\left(\frac{I_0}{I}\right)^{1/2},$$

where m_i is the ion mass. For lithium $m_i/m \approx 1.27\times10^4$, and, taking $I \approx 1.3\,\mathrm{kA}$, and $R \approx 1.3\times10^2\,\mu\mathrm{m}$, we find $\tau_{ion} \approx 44\,\mathrm{ps}$. This is about $10\times$ the bunch length and thus should be a small effect. [examine in more detail, particularly, aberrations could still be important]

In addition, in the underdense regime, a "transverse two-stream instability" may develop, and we will consider this in greater detail below.

The formation of the accelerating wakefield requires a backward acceleration of plasma electrons, and the usual picture of this return current sheath is that of a collisonless plasma, and excellent approximation on its face. However, in the collisionless limit, instabilities may *replace* collisions in dissipating the energy of the secondaries.[16] In particular, the two-stream (Buneman) instability will couple the electron motion to the ions

[13] Ref tunneling

[14] Ibid.

[15] F. J. Mehr and M. A. Biondi, Phys. Rev. **181**, 264 (1969).

[16] D. Prono, B. Ecker, N. Bergstrom, and J. Benford, Phys. Rev. Lett. **35**, 438 (1975); D. A. McArthur and J. W. Poukey, Phys. Rev. Lett. **27**, 1765 (1971).

on a time scale ν_{eiTS}^{-1}, where

$$\nu_{eiTS} = \frac{3^{1/2}}{2^{4/3}}\omega_p\left(\frac{m}{m_i}\right)^{1/3} \approx 3\times 10^{-2}\omega_p,$$

evaluating the result for lithium. For $n_p \approx 5\times 10^{14}\,\mathrm{cm}^{-3}$ this corresponds to $\nu_{eiTS}^{-1} \approx 26\,\mathrm{ps}$, and thus collisions should have only a small effect in dissipating the wakefield.

4. First-Order Optics for the Beam Midsection

Putting aside the higher-order effects mentioned in the previous section, let us consider in more detail the optics of the beam in the plasma. We distinguish between the beam-head, travelling through an overdense plasma, and the center portion of the beam, travelling through a channel denuded of plasma electrons. The beam head is treated in the next section.

One's first inclination is to seek incoming beam parameters so as to match the mid-section of the beam to the IFR focusing channel.[17] This would insure transport of the beam into the plasma without scalloping, filamentation and emittance growth. The optics attainable with the FFTB beamline indicate that the incoming beam cannot be focused to the requisite 2.7 μm at the entrance to the chamber; rather, one may expect $\sigma_x \approx \sigma_y \approx 50\ \mu\mathrm{m}$. Alternatively, one could contemplate employing the plasma for matching, by adiabatically tapering the plasma density profile. At the same time we should recognize that a simple mismatch itself can be dealt with, for sufficiently small energy spread; the circumstance that different portions of the beam see a different mismatch is however another matter, and demands a quantitative treatment. Let us first ask what would be required to match the beam at the beam peak.

The optics are described by

$$\frac{d^2\vec{r}_\perp}{ds^2} = -k_\beta^2\,\vec{r}_\perp,$$

with

$$k_\beta^2 = \frac{1}{2\gamma}k_p^2.$$

At 46.6 GeV and for $n_p = 10^{14} - 10^{15}\,\mathrm{cm}^{-3}$ we have $\lambda_\beta = 2\pi/k_\beta \approx 3.6\,\mathrm{cm}$ - $1.6\,\mathrm{cm}$ - $1.1\,\mathrm{cm}$.

The envelope equation takes the form

$$\frac{d^2\sigma_x}{dz^2} + k_\beta^2\sigma_x = \frac{\varepsilon_x^2}{\sigma_x^3},$$

and similarly for *y*. The various quantities are

$$\sigma_x^2 = \langle x^2\rangle - \langle x\rangle^2, \qquad \sigma_{xx'} = \langle x x'\rangle - \langle x\rangle\langle x'\rangle, \qquad \sigma_{x'}^2 = \langle x'^2\rangle - \langle x'\rangle^2,$$
$$\varepsilon_x^2 = \sigma_x^2\sigma_{x'}^2 - \sigma_{xx'}^2 = \left(\langle x^2\rangle - \langle x\rangle^2\right)\left(\langle x'^2\rangle - \langle x'\rangle^2\right) - \left(\langle x x'\rangle - \langle x\rangle\langle x'\rangle\right)^2.$$

[17] This said, one immediately realizes that the beam cannot be matched from a DC magnetic lattice in this sense, insofar as the focusing strength in the plasma varies along the beam. For matching, one would need rf quadrupole elements in the upstream lattice.

To numerically solve for the beam-size one needs only the beam spot-size specified at s=0 , together with the initial lattice parameters, β_0 and $\alpha_0 = -\beta_0'/2$. Other quantities needed are then,

$$\varepsilon_x = \sigma_x^2(s=0)/\beta_0, \qquad \frac{d\sigma_x}{ds}(s=0) = -\frac{\alpha_0}{\beta_0}\sigma_x(s=0).$$

[Numerical examples for $n_p = 5\times 10^{14}\,\mathrm{cm}^{-3}$].

5. First-Order Optics for the Beam Head

In this section, transport of a relativistic electron beam through an axially varying plasma much more dense than the beam is formulated and analyzed including the effects of head-to-tail misalignments and abberations. A nonlinear envelope formalism is derived involving a convolution over the beam. This model is valid in the regime of linear plasma response and a Gaussian beam (with waist varying in time and space) when the collisionless skin depth is not small compared to the spot-size. This formalism permits gridless multi-particle simulation of the plasma focus, and provides fast comparison for screen-oriented diagnostics. In reduced form the model permits real-time particle-less calculation of beam envelope and centroid evolution. This model is compared to the results of cloud-in-cell beam and fluid-plasma simulation for the case of an aligned beam.

Magnetically self-focused propagation of an electron beam in a plasma is one of the oldest problems in beam and plasma physics, dating back to the original work of Bennett,[18,19] Pierce[20], Bennett and Cox,[21] Buneman,[22] Hammer and Rostoker,[23] Lee and Sudan,[24] Thode and Sudan,[25] and Lee.[26] Experimental studies date to the work of Roberts and Bennett,[27] Graybill and Nablo,[28] and Graybill and Uglum.[29] Interest in the beam-plasma has stemmed from areas as diverse as astrophysics,[18,30] microwave generation,[20] ion-

[18] W. H. Bennett, "Magnetically Self-Focussing Streams," Phys. Rev. **45**, 890 (1934).

[19] W. H. Bennett, Phys. Rev. **98**, 1584 (1955).

[20] J. R. Pierce, *Travelling Wave Tubes*, (D. Van Nostrand, New York, 1950).

[21] J. L. Cox, Jr., and W. H. Bennett, Phys. Fluids **13**, 182 (1970).

[22] O. Buneman, Phys. Rev. **115**, 503 (1959).

[23] D. A. Hammer and N. Rostoker, Phys. Fluids **13**, 1831 (1970).

[24] R. Lee. and R. N. Sudan, Phys. Fluids **14**, 1213 (1971).

[25] L. E. Thode and R. N. Sudan, Phys. Fluids **18**, 1552 (1975), ibid. **18**, 1564 (1975), and L. E. Thode, ibid., **19**, 305 (1976), ibid., **19**, 831 (1976).

[26] E. P. Lee, Phys. Fluids **19**, 60 (1976).

[27] T. G. Roberts and W.H. Bennett, Plasma Phys. **10**, 381 (1968).

[28] S. E. Graybill and S. V. Nablo, "Observations of Magnetically Self-focusing Electron Streams," Appl. Phys. Lett **8**, 18 (1966).

[29] S. E. Graybill and J. R. Uglum, J. Appl. Phys. **41**, 236 (1970).

[30] H. Alfven, "On the Motion of Cosmic Rays in Interstellar Space," Phys. Rev. **55**, 425 (1935).

acceleration,[25] plasma-heating,[31,32] laser-pumping,[33] and military applications.[34] A number of review articles have been written over the years from some of these different perspectives.[35,36,37] The problem of interest here is simply optics.

At present theoretical models of beam optics in plasma consist of two extremes, one-dimensional thick lens models, and three-dimensional fully electromagnetic particle-in-cell simulations. While fully electromagnetic simulations are a useful arbiter among lesser models, there is a practical need to have a theoretical tool which permits rapid iterative design, and ultimately real-time results for comparison. In this section we set down and solve a wakefield formalism for plasma optics design. This formalism includes the important effect of abberrations (nonlinear focusing), and, for the first time, incorporates in a systematic way the effect of head-to-tail beam misalignments, as well as the self-consistent axial evolution of the beam in the plasma ("thick lens" effects). Application of this formalism sheds light on the question of misalignment amplification in a long pulse.

We proceed by formulating the dynamics of the beam-plasma assuming a cold-fluid linear plasma response. A wakefield formalism is derived, and for the case of no misalignment, is reduced to a nonlinear integrodifferential equation for the beam envelope. Next, the effect of misalignments is restored, analyzed, and reduced to a nonlinear beam break-up equation. Finally, we apply this model to the case of E157.

Wakefields in the Linear Regime

We consider propagation of a relativistic beam in the *z*-direction into an initially quasineutral plasma with initial density uniform in the *x-y* plane. In the limit that the plasma is much denser than the beam, and for sufficiently small times, the plasma response is governed by the linearized cold fluid equations.

$$\frac{\partial \rho_{e1}}{\partial t} + \vec{\nabla} \bullet \left(\rho_{e0} \vec{V}\right) = 0, \tag{1}$$

$$\frac{\partial \vec{V}}{\partial t} = \vec{\nabla}\, \phi + \frac{1}{c}\frac{\partial \vec{a}}{\partial t} - \nu\, \vec{V}, \tag{2}$$

where the scalar and vector potentials in the Lorentz gauge are ϕ, and $\vec{a}$, and are dimensionless after a normalization by e/mc^2. The electron charge is $-e$, the electron mass is m and c is the speed of light. The plasma electron velocity is $\vec{V} = \vec{\beta} c$, the initial plasma electron charge density is ρ_{e0}, and the perturbation is ρ_{e1}. We model collisions with a constant collision rate ν. We change coordinates from z, t to z and $\zeta = ct - z$, and assume that the beam charge density $\rho_b(\vec{r}_\perp, z, \zeta) = 0$ for $z<0$. We also assume z-variation at fixed z is

[31] D. A. MacArthur and J. W. Poukey, Phys. Rev. Lett. **27**, 1765 (1971).

[32] D. Prono, B. Ecker, N. Bergstrom, and J. Benford, Phys. Rev. Lett. **35**, 438 (1975).

[33] Yu. V. Tkach, Ya. B. Fainberg, I. I. Magda, G. V. Skachek, S. S. Pushkarev, and N. I. Gaponenko, Sov. J. Plasma Physics. **2**, 259 (1976).

[34] D. Birx, "Induction Linear Accelerators", *Proceedings of the U. S. Particle Accelerator School*, edited by Melvin Month (AIP, New York, 1989).

[35] R. Okamura, Y. Nakamura, and N. Kawashima, Plasma Phys. **19**, 997 (1977). This excellent review covers the basic features and applications of beam-plasma physics, together with a discussion of an experiment using short-pulse REBs (1 ns pulse, 500 keV energy, 2 kA current) for plasma heating.

[36] G. Wallis, K Sauer, D. Sunder, S. E. Rosinskii, A. A. Rukhadze and V. G. Rukhlin, Sov. Phys.-Usp. **17**, 492 (1975).

[37] P. C. de Jagher, F. W. Sluijter, and H. J. Hopman, Physics Reports **167**, 177 (1988).

small on the scale of a plasma skin depth ("frozen-field" approximation). In this case, Laplace transforming in z we have,

$$\beta_z = \frac{p}{p+\nu}\psi, \tag{3}$$

$$\vec{\beta}_\perp = \frac{1}{p+\nu}\vec{\nabla}_\perp\phi + \frac{p}{p+\nu}\vec{a}_\perp, \tag{4}$$

$$\rho_{e1} = -\frac{\rho_{e0}}{p(p+\nu)}\nabla_\perp^2\phi - \frac{1}{p}\vec{\beta}_\perp \bullet \vec{\nabla}_\perp\rho_{e0}, \tag{5}$$

where the "pinch" potential is $\psi = a_z - \phi$, and the gauge condition $\vec{\nabla}_\perp \bullet \vec{a}_\perp = p\psi$ has been employed. The gradient in the transverse coordinates is $\vec{\nabla}_\perp$. The transverse fluid velocity is $\vec{\beta}_\perp$ and the axial velocity is β_z, all normalized by c.

The potentials are determined from Maxwell's equations which may be expressed, after substitutions from Eqs. (1)-(3), as

$$\vec{\nabla}_\perp \bullet \left(\varepsilon\vec{\nabla}_\perp\phi\right) = -\frac{4\pi e}{mc^2}\rho_b - p\vec{a}_\perp \bullet \vec{\nabla}_\perp\varepsilon, \tag{6}$$

$$\left(\nabla_\perp^2 - \omega_e^2\frac{p}{p+\nu}\right)\psi = -\frac{4\pi e}{mc^2}\rho_b\frac{\varepsilon-1}{\varepsilon} + \left(\vec{\nabla}_\perp\phi + p\vec{a}_\perp\right)\bullet\frac{\vec{\nabla}_\perp\varepsilon}{\varepsilon}, \tag{7}$$

$$\left(\nabla_\perp^2 - \omega_e^2\frac{p}{p+\nu}\right)\vec{a}_\perp = p(\varepsilon-1)\vec{\nabla}_\perp\phi. \tag{8}$$

Here $\nabla_\perp^2$ denotes the Laplacian in the transverse coordinates and the dielectric function is

$$\varepsilon = 1 + \frac{\omega_e^2}{p(p+\nu)+\omega_e^2} \tag{9}$$

Retardation has been neglected assuming that $|pb/\gamma| << 1$ and $|p/\gamma| << \omega_e$, where γ is the Lorentz factor for the beam, and ω_e is the angular plasma frequency in units of cm^{-1}, $\omega_e^2 = 4\pi n_e e^2/mc^2$. Since we are primarily interested in frequencies $|p| \sim O(\omega_e)$, and small skin depths this is a fair approximation for a relativistic beam. Radial beam currents are assumed negligible, thus "sausaging" ("breathing", "scalloping") of the beam is neglected. Note that the induced transverse vector potential is of order $O(\omega_e a)^2$ smaller than the electrostatic and pinch potentials in this limit, and thus is negligible.

For the remainder of this section we specialize to the collisionless limit, and consider perturbations to an initially uniform plasma, so that $\vec{\nabla}_\perp\varepsilon = 0$. The formal solution for ψ is, after an inverse Laplace transform,

$$\psi(\vec{r}_\perp, z, \zeta) = \int_0^\zeta d\zeta' \omega_e(z)\sin\left\{\omega_e(z)(\zeta-\zeta')\right\}\Psi(\vec{r}_\perp, z, \zeta'), \tag{10}$$

where

$$\Psi(\vec{r}_\perp, z, \zeta') = \frac{e}{mc^2}\int d^2\vec{r}_\perp' G(\vec{r}_\perp, \vec{r}_\perp')\rho_b(\vec{r}_\perp', z, \zeta'). \tag{11}$$

For boundary conditions at infinity the Green's function is just,

$$G(r, r', \varphi, \varphi') = -2\sum \exp\{im(\varphi - \varphi')\} I_m(\omega_e r_<) K_m(\omega_e r_>), \tag{12}$$

with ρ and φ polar coordinates in the transverse plane.

Beam Motion

In the limit of large plasma skin-depth the motion of beam particles is governed solely by the pinch potential of Eq. (). The Hamiltonian takes the form

$$H = \gamma + \frac{1}{2\gamma} + \frac{p_\perp^2}{2\gamma} + \psi, \tag{13}$$

and the transverse and longitudinal motion are governed by

$$\frac{d}{dz}\gamma\frac{d\vec{r}}{dz} = -\nabla_\perp \psi, \tag{14}$$

$$\frac{d\gamma}{dz} = \frac{\partial\psi}{\partial\zeta}. \tag{15}$$

Equations (8), (11) and (12) provide a complete description of beam propagation in overdense plasma in the large skin-depth limit.

Gaussian Beam Approximation

Equation (8) is further simplified by assuming that the beam is initially Gaussian, and maintains a Gaussian profile,

$$\rho_b(\vec{r}_\perp, z, \zeta) = \frac{1}{c}\frac{I(\zeta)}{\pi a(z,\zeta)^2}\exp\{-u^2(\vec{r}_\perp, z, \zeta)\}, \tag{16}$$

where

$$\vec{u} = \frac{\vec{r}_\perp - \vec{\xi}(z,\zeta)}{a(z,\zeta)}, \tag{17}$$

I is the beam current, $a(z,z)$ is the beam spot-size, and $\vec{\xi}(z,\zeta)$ is the beam centroid. Using Eq. (13), Eqs. (8) and (9) may be combined and simplified to reveal

$$\Psi(\vec{r}_\perp, z, \zeta') = -2\nu(\zeta)\vartheta\left(u^2(\vec{r}_\perp, z, \zeta), \omega_e^2 a^2(\vec{r}_\perp, z, \zeta)\right), \tag{18}$$

where $\nu = I/I_0$ is a normalized current (Budker's parameter), with $I_0 = mc^3/e \sim 17$ kA, and

$$\vartheta(a,b) = K_0\left(\sqrt{ab}\right)\int_0^a d\mu I_0\left(\sqrt{\mu b}\right)e^{-\mu} + I_0\left(\sqrt{ab}\right)\int_a d\mu K_0\left(\sqrt{\mu b}\right)e^{-\mu}$$
$$\approx -\frac{1}{2}\left\{\log\left(\frac{ab}{4}e^{2C}\right) + E_1(a)\right\} \tag{19}$$

The quantity C~0.5772 is Euler's constant. The approximate expression in Eq. (16) is valid for small b, and is compared to the exact result in Fig. . The function E_1 is the exponential integral $E_1(a) = \int_a d\mu\, e^{-\mu}/\mu$. The result for Ψ is then,

$$\Psi(\vec{r}_\perp, z, \zeta') \approx \nu(\zeta)\left[2\log\left(\frac{e^C}{2}u\,\omega_e a\right) + E_1(u^2)\right]_{(\vec{r}_\perp, z, \zeta')} \tag{20}$$

With these results we can make more explicit the force terms in Eqs. (10) and (11). The longitudinal wakefield is

$$\frac{\partial\psi}{\partial\zeta}(\vec{r}_\perp, z, \zeta) = \int_0^\zeta d\zeta'\omega_e^2(z)\cos\left\{\omega_e(z)(\zeta-\zeta')\right\}\Psi(\vec{r}_\perp, z, \zeta') \tag{21}$$

while the transverse wakefield is

$$\nabla_\perp\psi(\vec{r}_\perp, z, \zeta) = \int_0^\zeta d\zeta'\omega_e(z)\sin\left\{\omega_e(z)(\zeta-\zeta')\right\}\nabla_\perp\phi_b(\vec{r}_\perp, z, \zeta'), \tag{22}$$

with ϕ_b the vacuum electrostatic potential of the beam,

$$\nabla_\perp\phi_b(\vec{r}_\perp, z, \zeta) = 2\frac{\nu(\zeta)}{a(z,\zeta)}\left\{1-\exp\left\{-u^2\right\}\right\}\frac{\vec{u}}{u^2} \quad , \tag{23}$$

To close this system of equations one requires a prescription for computing the centroid and spot-size from the particle ensemble. These are

$$\vec{\xi}(z,\zeta) = \left\langle \vec{r}_\perp \right\rangle\Big|_{(z,\zeta)} \tag{24}$$
$$a^2(z,\zeta) = \left\langle r_\perp^2 \right\rangle\Big|_{(z,\zeta)} - \xi^2(z,\zeta). \tag{25}$$

where the brackets denote an average over a beam slice. Equations (11) and (14)-(16) provide a complete description of beam optics in the plasma, including misalignments and the effect of abberations.

Envelope Model (No Misalignment)

In the case of no beam misalignment (x=0 or constant along the beam) one final simplification is immediately evident. Differentiating Eq.(16) twice and substituting from Eq. (11) one arrives at the envelope equation,

$$\frac{\partial^2 a}{\partial z^2} + \frac{\langle \vec{r}_\perp \bullet \nabla_\perp \psi \rangle}{\gamma a} - \frac{\varepsilon^2}{a^3} = 0, \tag{26}$$

with ε the edge emittance (twice the rms). Computing the indicated ensemble average as an average over radius weighted by the charge density of Eq.(13), one finds

$$\left\{ \frac{\partial^2}{\partial z^2} + \kappa^2(z,\zeta) \right\} a(z,\zeta) = \frac{\varepsilon^2}{a^3(z,\zeta)}, \tag{27}$$

where

$$\kappa^2(z,\zeta) = \frac{2}{\gamma} \int_0^\zeta d\zeta' \omega_e(z) \sin\{\omega_e(z)(\zeta - \zeta')\} \frac{\nu(\zeta')}{a^2(z,\zeta) + a^2(z,\zeta')}. \tag{28}$$

Equation (18) provides a complete description of beam optics in the absence of misalignments. To numerically solve Eq.(18) one needs only the beam spot-size specified at z=0 for all z, together with the initial lattice parameters, β_0 and β_0' . Other quantities needed are then,

$$\varepsilon = a^2(z=0,\zeta)/\beta_0, \tag{29}$$

$$\frac{\partial a}{\partial z}(z=0,\zeta) = \frac{\beta_0'}{2\beta_0} a(z=0,\zeta). \tag{30}$$

Any numerical solution must also check the consistency of the assumptions made above, in particular the linearity of the plasma response, and the assumption $k_e a$<<1.

For the examples, we take

$$\nu(\zeta) = \nu_m \exp\left\{ -\frac{(\zeta - \zeta_0)^2}{2\sigma_z^2} \right\}, \tag{31}$$

with σ_z the rms length of the beam, and ζ_0 chosen to be a few σ_z. To accurately sample the sinusoidal wakefield with a second order integration the number of points required in z is about 20 per plasma period; for a long plasma period, about 20 points are required to accurately resolve the Gaussian bunch shaper. For the axial advance we use a fourth-order Runge-Kutta differencing, with constant step-size in vacuum regions, and step-size varying as $1/\omega_e$ within the plasma. For a typical run, 30 steps in z are required. The simulation BEAP follows both the envelope equation of Eq. (27), and the multiparticle motion described by Eqs. (14) - (15), and thus allows easy comparison of the two models. Description of the particle initialization is relegated to the discussion of Sec. IV, as the details are not crucial to the results of this gridless simulation.

[Discuss simulation results here]

6. Particle-in-Cell Simulation

To check the results of Secs. 4 and 5, we resort to a particle-in-cell simulation. The simulation used has been described elsewhere.[38] For this tech. note, we excerpt the description given in the reference.

[38] D.H. Whittum, "Transverse two-stream instability of a beam with a Bennett profile", *Phys. Plasma* **4** (1997) 1154.

The PIC simulation divides the beam into N_t ~30 x ($\omega_e\tau/2\pi$) slices and each beam slice is modelled by N~4096-16384 macroparticles. Each slice is initialized at z=0 with a Bennett distribution making use of symmetrized Hammersley deviates along the lines of previous work.[39] The beam particle motion in transverse position $\vec{r}_\perp$ and momentum $\vec{p}_\perp$ (normalized by mc) is governed by the pinch gradient

$$\frac{d\vec{r}_\perp}{dz} = \frac{\vec{p}_\perp}{p_z}, \qquad \frac{d\vec{p}_\perp}{dz} = -\vec{\nabla}_\perp \psi,$$

and these equations are advanced in z with a leap-frog algorithm,[18] with p_z constant, and no slippage in t.

As for the plasma electrons, one "slice" of M~4096-65536 plasma macroparticles is initialized for each step in z, and passed through the beam from the head to the tail. The plasma initialization loads $M/2$ pairs (x,y) uniformly within the unit circle, by rejection, and quiets the loading by reflection through the origin.[18] This loading subsequently can be deformed to a cut-off Bennett profile. Plasma particle momenta were initialized to zero. The plasma advance is a leap-frog in the beam coordinate t, governed solely by the electrostatic potential,

$$\frac{d\vec{r}_\perp}{d\tau} = \vec{p}_\perp, \qquad \frac{d\vec{p}_\perp}{d\tau} = \vec{\nabla}_\perp \phi,$$

The initial quasineutral equilibrium is achieved by adiabatic relaxation of the initially uniform plasma in the potential of an undisplaced beam. Typical beam displacements are 10^{-5}-10^{-4} beam radii, small enough to observe saturation prior to strong nonlinearity, and large enough to avoid problems with round-off error.

The potentials are determined from the reduced Maxwell's equations,

$$\nabla_\perp^2 \phi = -\frac{4\pi e}{mc^2}\left(\rho_b + \rho_e + \rho_i\right), \qquad \nabla_\perp^2 A = -\frac{4\pi e}{mc^2}\rho_b.$$

Charge allocation and field interpolation is performed by area-weighting in x-y. These are solved by a fast Fourier transform in x, with periodic boundary conditions, and a finite difference solution in y, with open boundary conditions. Sensitivity to these somewhat artificial boundary conditions was gauged by varying the size of the mesh, and by comparison with three other choices of boundary conditions: periodic in x and y, conducting in x and y, conducting in x and open in y. For boundaries displaced by 10-20 beam radii there is no remarkable dependence on boundary conditions.

7. Studies

[to be continued]

8. Conclusions

[to be continued]

[39] D. H. Whittum, "Cumulative hose instabilities of a magnetically self-focused slab electron beam", *Phys. Fluids* **B** 5, 4432 (1993).